Earthquake Geotechnical Engineering for Protection and Development of Environment and Constructions – Silvestri & Moraci (Eds)
© 2019 Associazione Geotecnica Italiana, Rome, Italy, ISBN 978-0-367-14328-2

Seismic shear behavior of clayey volcanic soil in residential area damaged by the 2016 Kumamoto earthquakes in Japan

S. Izumiya, A. Kamura & M. Kazama
Tohoku University, Sendai, Miyagi, Japan

J. Kim
Korea Institute of Civil Engineering and Building Technology, Gyeonggi-do, Korea

S. Sato
Fukken Gijutsu Consultant, Sendai, Miyagi, Japan

ABSTRACT: Sandy volcanic soils, including pumice, are vulnerable to earthquakes. On the contrary, clayey soil does not liquefy and is stronger than sandy soil. However, during the 2016 Kumamoto earthquake, a large ground deformation occurred in the residential area of Mashiki Town wherein clayey volcanic soil was deposited. We studied the seismic shear behavior of this clayey volcanic soil using a torsional cyclic shear test with a random shear stress history corresponding to actual seismic records. In our test, we also studied the effects of a series of seismic motion histories and the initial shear stress because most damage occurred on the slope area. As a result, in the case with initial shear stress owing to the slope, a larger residual strain developed compared to the case without an initial shear stress.

1 INTRODUCTION

It is well known that volcanic ash and sandy soils are vulnerable to earthquakes because sandy volcanic soils can easily liquefy during earthquakes (Volcanic Rocks and Soils, 2015; Kazama et al. 2006; Orense et al. 2006). In contrast, the ground in Mashiki Town, Kumamoto Prefecture, is composed of clayey volcanic soil. Figure 1 shows the damage distribution of the 2016 Kumamoto earthquake, sampling points, and the strong ground motion observation station. This area is covered with clayey volcanic soil from the Aso volcano. This soil is called Haido, and in this area, it is deposited up to a thickness of approximately 10 m. According to a field investigation by Hashimoto and Matsushita (2017), most damage occurred on the slope area, and the larger the slope, the greater was the ground deformation. On the contrary, Chiaro et al. (2012) performed a laboratory test focusing on the relation between the initial shear stress and the liquefaction strength and observed that the presence of initial static shear (i.e. sloping ground condition) can be either detrimental or beneficial to cyclic resistance.

There is another damage feature concerning the occurrence of an earthquake. Table 1 shows places wherein the 2016 Kumamoto earthquake had a magnitude (M_{JMA}) of 5.0 or higher. Figure 2 shows the time history of seismic waves observed at the KiK-net Mashiki observation station during the 2016 Kumamoto earthquakes. These earthquakes, each with a magnitude of 5.0 or higher, occurred six times in 30 h, and the peak ground acceleration (PGA) reached 1156.9 Gal for the main shock, as recorded at the KiK-net Mashiki observation station.

Based on the earthquake disaster features described above, we investigated the cyclic shear behavior of clayey volcanic soil after this series of earthquakes and studied the influence of the initial shear stress owing to the slope angle on the degree of residual deformation.

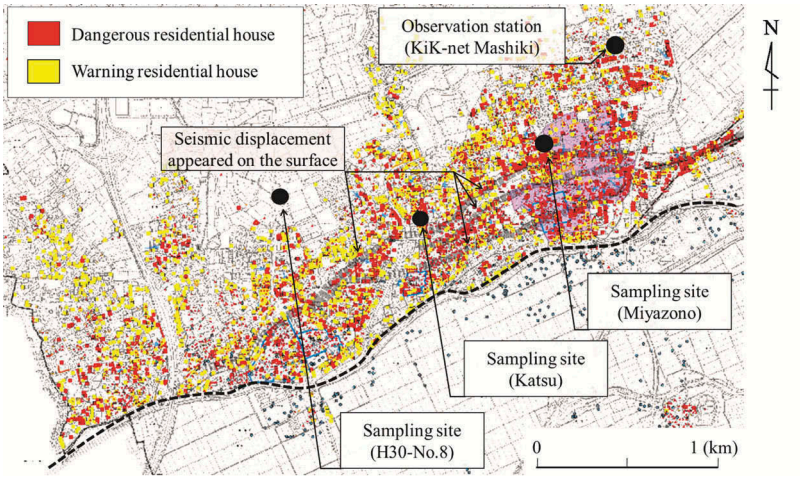

Figure 1. The damage distribution, sampling points, and the strong ground motion observation station

Table 1. Earthquakes of JMA Magnitude 5.0 or more in the 2016 Kumamoto earthquakes.

Event	Date and Time of occurrence	Magnitude (M_{JMA})	Seismic Intensity (JMA)	PGA (Gal)
1	14th April at 09:26 P.M.	6.5	7	925.0
2	14th April at 10:07 P.M.	5.8	lower 6	559.8
3	15th April at 00:03 A.M.	6.4	upper 6	590.2
4	15th April at 00:06 A.M.	5.0	upper 5	189.1
5	16th April at 01:25 A.M.	7.3(Main shock)	7	1156.9
6	16th April at 01:45 A.M.	5.9	lower 6	384.5

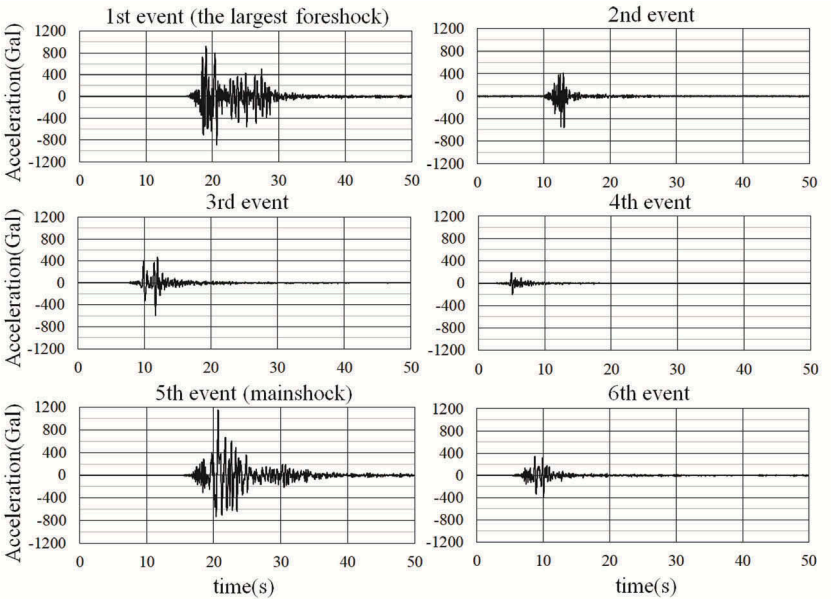

Figure 2. Time history of seismic waves observed at the KiK-net Mashiki observation station during the 2016 Kumamoto earthquakes.

2 SAMPLES

The tests used clayey volcanic soil sampled at Mashiki Town. Figure 3 shows the soil profiles at the sampling site. The red bar denotes the depth used for the tests. Each sample comprised unsaturated soil from a depth shallower than the groundwater level (groundwater level of Miyazono: G.L. -10 m, Katsu: G.L. -5.6 m, H30-No.8: G.L. -9.8 m). Table 2 lists the physical properties of the samples, and Figure 4 shows the grain-size accumulation curves. The liquid limits were estimated by fall cone tests in consideration of the influence of the gravel. The samples are clayey volcanic soil called Haido. The sensitivity ratio was very high and the natural water content was higher than the liquid limit, as shown in Table 2.

Picture 1 shows the samples with the undisturbed and disturbed conditions (These are the same samples). In appearance, the undisturbed sample did not seem to contain water. However, once disturbed, moisture seeped out of the sample, and the sample became muddy.

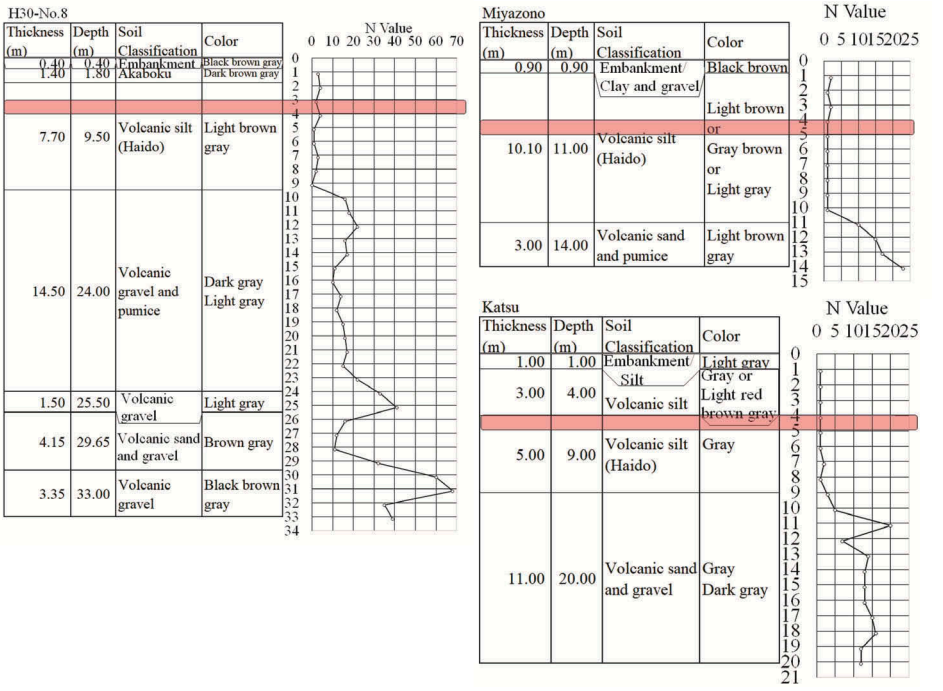

Figure 3. Soil profiles at the sampling site

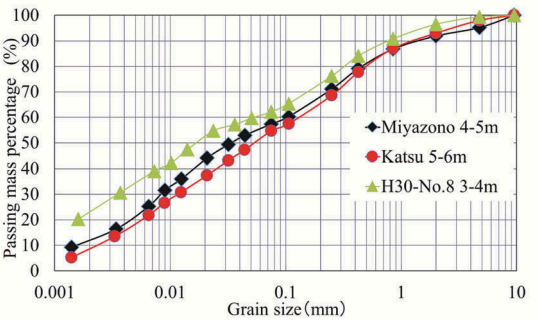

Figure 4. Grain size accumulation curves

Picture 1. Soil materials tested. From the left: Undisturbed sample, Disturbed sample.

Table 2. Physical properties of soils sampled

Sample Name (Depth)	Water Content (%)	Particle Density (g/cm^3)	Liquid Limit (fall cone) (%)	Plastic Limit (%)	Soil Classification (USCS)
Miyazono 4-5 m	86.2	2.682	66.9	44.8	MH
H30-No.8 3-4 m	75.6	2.670	67.1	44.6	MH
Katsu 5-6 m	81.1	2.676	62.2	46.2	MH

L.L. is estimated from Fall Cone Test

It has also been reported that Haido is greatly affected by disturbance, having a dynamic strength ratio comparable to that of Kuroboku soil and Kanto loam and that the dynamic strength increases with an increase in the initial shear stress ratio (Nagase et al. 1997).

3 OUTLINE OF UNDRAINED CYCLIC SHEAR TEST USING RANDOM STRESS RATIO HISTORY ESTIMATED FROM SEISMIC WAVEFORM

We carried out a hollow torsional test using random stress waves estimated from the seismic waveform of the 2016 Kumamoto earthquakes observed at the KiK-net observation station. For the sake of simplicity, the shear stress ratio used for the cyclic shear test was assumed to be proportional to the observed seismic acceleration history.

Given this assumption, the contribution to the shear stress ratio of the short-period component of acceleration will be overestimated (Kazama, 1999); however, because there is ambiguity of the seismic motion here at the investigation point, the seismic acceleration history was handled as it corresponded to the ground's shear stress ratio. In addition, the amplitude of the shear stress wave used for the cyclic shearing was calculated from the maximum acceleration α_{max} of the earthquake-record-based calculation formula (1) of equivalent cyclic shear stress amplitude ratio of the Recommendation for Design of Building Foundations (Architectural Institute of Japan, 1988).

$$\frac{\tau_d}{\sigma_z'} = \gamma_n \frac{\alpha_{max}}{g} \frac{\sigma_z}{\sigma_z'} \gamma_d \tag{1}$$

where $\gamma_n = 0.1 \times (M - 1)$; $\gamma_d = (1 - 0.015z)$, M = Magnitude (main shock $M = 7.3$, aftershock $M = 5.9$), and z = depth from surface (m).

Considering that the test involves isotropic consolidation, the effective stress was calculated by multiplying the overburden pressure by 2/3[1]. A hollow specimen having outer diameter of 6.5 cm, inner diameter of 3 cm, and height of 10 cm was prepared by a trimming method. The membrane thickness was 0.3 mm.

1. Assuming coefficient of earth pressure $K_0 = 0.5$, mean effective stress $p' = \frac{\sigma_v' + 2K_0\sigma_v'}{3} = \frac{2}{3}\sigma_v$

Table 3. Experimental conditions of undrained cyclic shear

Case	Sample Point and Depth	Confining Pressure (kPa)	Slope Angle (degree)	Peak Shear Stress Ratio (kPa)	Input Stress Wave
Kim method	Miyazono 4-5 m	45	0	0.4	Described in chapter 4.1
Actual	H30-No.8 3-4 m	35	0	1.027	All waves of Table 1
I0D	Katsu 5-6 m	55	0	1.023	The main shock
I+5D	Katsu 5-6 m	55	5	1.153	The main shock
I−5D	Katsu 5-6 m	55	−5	0.893	The main shock

Table 3 lists the experimental conditions. Case Kim method is a test method proposed by Kim et al. (2017): a shear test aimed at evaluating the residual deformation performance of soil subjected to a large earthquake. Case Actual investigated the influence of foreshocks on the damage caused by the main shock by loading multiple seismic waves continuously and then loading the main shock. Cases I0D, I+5D and I−5D changed the initial shear stress in consideration of the inclination of the ground surface and investigated the influence on the deformation owing to the inclination. The initial shear stress τ_0 was calculated by equation (2).

$$\tau_0 = \gamma_t z \cos i \sin i \tag{2}$$

where γ_t is the wet unit weight of the soil and i is the angle of the slope.

The inclination was considered as the representative value of an in situ average inclination degree of 5. The stress ratio was ±0.13. The positive and negative values of the inclination and initial shear stress correspond to the positive or negative values of the input waves. The cases which reached the values of shear strain 15% during monotonic loading process and 30% during cyclic loading process were regarded as the limit state in the experiment.

4 TEST RESULTS AND DISCUSSION

4.1 *Evaluation of residual deformation performance by cyclic shearing of Haido*

Figure 5 shows the stress ratio–shear strain relationship and the mean effective stress path for the method proposed in the Case Kim method. According to the test method proposed by

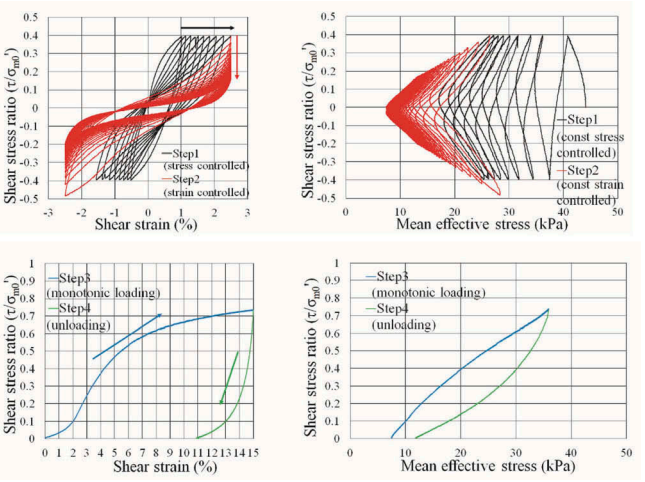

Figure 5. Shear stress ratio–shear strain relationship and mean effective stress path in the Case Kim method

Kim et al. (2017), first, cyclic loading with a constant shear stress ratio is performed as Step 1, and the constant shear strain test is then performed as Step 2. After that, monotonic loading is performed as Step 3. Finally, unloading is performed as Step 4.

In this research, the set value of the stress ratio in Step 1 was 0.4, and the shear strain amplitude in Step 2 was set to 2.5%. A stress ratio of 0.4 is the stress ratio assuming a Level-2 earthquake ground motion in view of the 2016 Kumamoto earthquakes. Focusing on Step 1, the shear strain reached 2.5% after 9 cycles with a stress ratio of 0.4. In Step 2, after 23 cycles, the loop became steady and ended.

The shear stress ratio when the shear strain reached 2.5% in the loading loop just before termination was approximately 0.17. Compared to immediately after switching to Step 2, the shear modulus was reduced by approximately 60%, which was approximately 83% lower than that when loading the first wave in Step 1. Compared to the state before loading, the effective stress decreased by approximately 60% at the end of Step 1 and by approximately 83% at the end of Step 2.

After cyclic loading as Step 3, monotonic loading was performed until the shear strain reached 15%. Then, as Step 4, unloading was performed until the stress ratio became 0 and was drained. During monotonic loading, the shear stress increased as the shear strain increased, and reached a shear stress ratio of 0.73 when the shear strain was 15%. Approximately 11% of the residual shear strain occurred after unloading.

Kim et al. (2017) classified the soil as "No Liquefaction," "Limited Damage," or "Catastrophic Damage" by this test method. A series of test results shows that this sample is a cohesive soil whose stiffness does not suddenly decrease. The sample is classified as "Limited Damage." Upon receiving large shear stress, the excess pore water pressure rises and the effective stress decreases, but the reduction in the secant shear modulus is approximately half. Thus, it can be said that this soil sample does not lead to brittle fractures.

4.2 *Influence on deformation by multiple earthquakes*

Figure 6 shows the time history of shear stress ratio, shear strain, and excess pore water pressure ratio in Case Actual. This time history is shown corresponding to the step of control in the test of the input seismic shear stress, and one controlling step corresponds to in-situ 0.01 s. The shear strain and the excess pore water pressure ratio increased greatly at time of the largest foreshock (the first event) and the mainshock (the fifth event), the JMA seismic intensity level of those earthquakes were 7. However, the other events had little effect on the development of the pore water pressure and the shear strain. These results indicate that the first foreshock and the mainshock were the main causes of the slope deformation at Mashiki town.

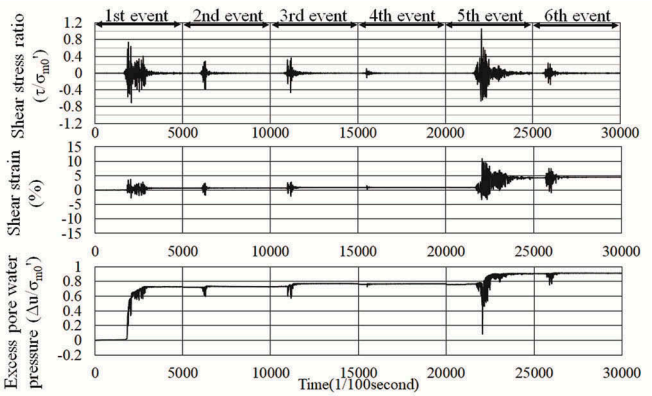

Figure 6. Time history of shear stress ratio, shear strain, and excess pore water pressure ratio in Case Actual

4.3 *Influence on residual deformation by slope*

Figure 7 shows the stress ratio–shear strain relationship and the mean effective stress path. In addition, Figure 8 shows the time history of the shear stress ratio, shear strain, and excess pore water pressure ratio in Case I0D, I+5D, and I-5D. In Case I0D, which did not have an initial shear stress, the shear strain reached 21.1% at the peak, but continued to exert stress without strain softening. The residual shear strain after loading was 4.9%.

In contrast, in Case I+5D, which applied a positive initial shear stress, the shear strain reached 30% without reaching the peak value of the stress ratio on the way, so the test was terminated at that point. From the stress ratio–shear strain relationship, it is considered that no further increase in shear stress can be expected even if the shear strain is further increased.

In Case I-5D with a negative initial shear stress, the shear strain in the positive direction was 17.5%, which was the lowest among the three cases. However, the shear strain in the negative direction was -19.8%, which was considerably large compared to -3.8% without an initial shear case. The residual shear strain was -17.5%, which was more than 3.5 times larger than that in Case I0D.

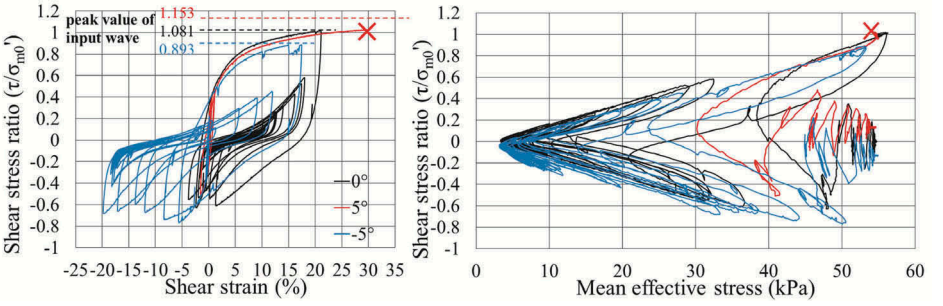

Figure 7. Shear stress ratio–shear strain relationship and mean effective stress path in Cases I0D to I-5D

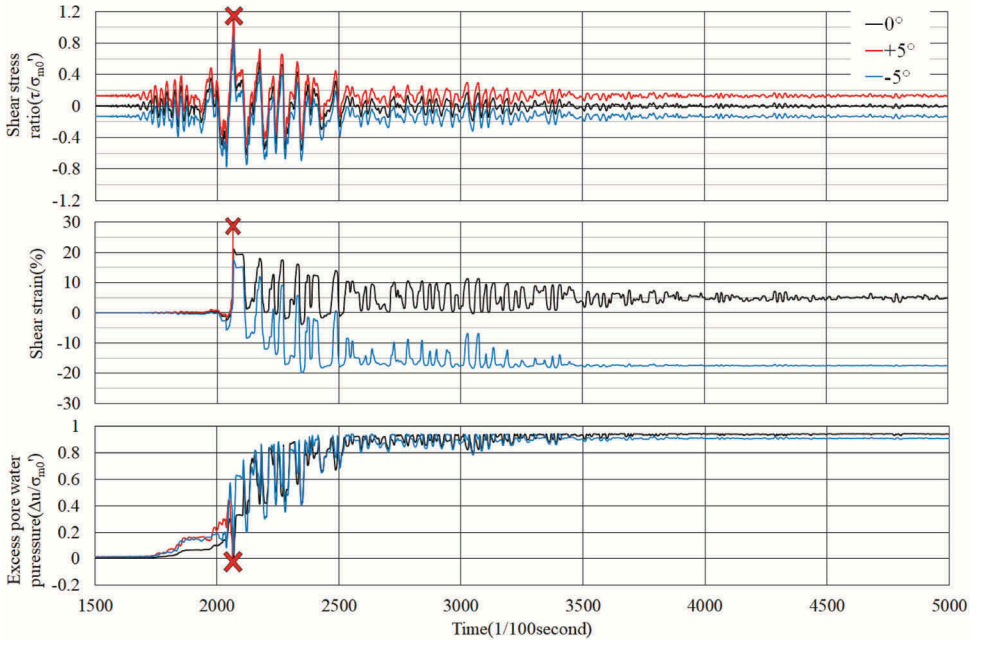

Figure 8. Time history of shear stress ratio, shear strain, and excess pore water pressure ratio in Cases I0D to I-5D.

From the abovementioned cases, it is clear that the strain gradually develops under the inclined slope with the shear stress of the earthquake. This result is consistent with the situation at the site in which significant damage occurred on the slope. This damage pattern can be attributable to clayey volcanic soils, considering the knowledge of the deformation property of sandy soils subject to cyclic loading with an initial shear stress (Hyodo et al. 1991)

5 CONCLUSION

In this research, we conducted undrained cyclic shear tests using clayey volcanic soil sampled from Mashiki Town and obtained the following results:

1. Using the new test procedure to assess the residual deformation potential proposed by Kim et al. (2017), the clayey volcanic soil of the damaged area is classified as soil with "Limited Damage" potential.
2. We studied the cyclic shear behavior of the clayey volcanic soil using a random seismic shear history corresponding to the actual seismic record observed at Mashiki Town. As a result, the soil endured a peak shear stress ratio as large as the actual seismic load. However, the pore pressure generated and the effective stress decreased to approximately 10% of the initial effective stress.
3. Regarding the effects of the six historic seismic events, the shear strain and the excess pore water pressure ratio increased greatly at the time of the largest foreshock (the first event) and the mainshock (the fifth event). However, the other events had little effect.
4. When comparing the influence of the slope by changing the initial shear stress, a larger residual strain developed when the initial shear stress was applied corresponding to the slope angle.

ACKNOWLEDGMENTS

In this research, Kabuki technical staff tested the physical properties. In addition, we used the earthquake records of the KiK-net observation station. We are grateful for the assistance. This study was supported by JSPS KAKENHI Grant Number 16H02362.

REFERENCES

Architectural Institute of Japan. 1988. Recommendations for Design of Building Foundations: 165

Hashimoto T. and Matsushita K. 2017. Analysis of residential area and building damage in Mashiki town at the 2016 Kumamoto earthquake using GIS. *GeoKanto 2017*: 297-300.

Chiaro G., Koseki J. and Sato T. 2012. Effects of initial static shear on liquefaction and large deformation properties of loose saturated Toyoura sand in undrained cyclic torsional shear tests. *Soil and Foundations*, 52(3): 498-510.

Hyodo M., Murata H., Yasufuku N. and Fujii T. 1991. Undrained cyclic shear strength and residual shear strain of saturated sand by cyclic triaxial tests. *Soil and Foundations*, 31(3): 60-76.

Kazama M. 1999. Reconsideration of the Shear Stress Ratio Generated by Earthquakes. *Soil mechanics and foundation engineering*, 47(6): 13-16 (in Japanese).

Kazama M., Takamura H., Unno T., Sento N. and Uzuoka R. 2006. Liquefaction mechanism of unsaturated volcanic sandy soil. *Journal of Japan Society of Civil Engineers C* 62(2): 546-561.

Kim J., Kawai T. and Kazama M. 2017. Laboratory testing procedure to assess post-liquefaction deformation potential. *Soils and Foundations*, 57(6): 905-919.

Nagase H., Hirooka A., Tanoue Y. and Kuriya Y. 1997. Dynamic deformation and strength characteristics of three unusual soils in Kyushu. *Proceedings of the JSCE earthquake engineering symposium*, 24: 429-432.

Orense R., Zapanta A., Hata A. and Towhata I. 2006. Geotechnical characteristics of volcanic soils taken from recent eruptions. *Geotechnical and Geological Engineering*, 24: 129-161.

Rotonda T., Cecconi M., Silvestri F. Tommasi P. 2015. *Volcanic Rock and Soils*. Boca Raton: CRC Press.